ARTICLES
PUBLISHED ONLINE: 9 NOVEMBER 2008 | DOI: 10.1038/NMAT2317
nature materials

A metal-free polymeric photocatalyst for hydrogen production from water under visible light

Xinchen Wang[1,2]*, Kazuhiko Maeda[3], Arne Thomas[1], Kazuhiro Takanabe[3], Gang Xin[3], Johan M. Carlsson[4], Kazunari Domen[3]* and Markus Antonietti[1]

The production of hydrogen from water using a catalyst and solar energy is an ideal future energy source, independent of fossil reserves. For an economical use of water and solar energy, catalysts that are sufficiently efficient, stable, inexpensive and capable of harvesting light are required. Here, we show that an abundant material, polymeric carbon nitride, can produce hydrogen from water under visible-light irradiation in the presence of a sacrificial donor. Contrary to other conducting polymer semiconductors, carbon nitride is chemically and thermally stable and does not rely on complicated device manufacturing. The results represent an important first step towards photosynthesis in general where artificial conjugated polymer semiconductors can be used as energy transducers.

The search for suitable semiconductors as photocatalysts for the splitting of water into hydrogen gas using solar energy is one of the noble missions of material science. An optimal material would combine an ability to dissociate the water molecules, having a bandgap that absorbs light in the visible range and to remain stable in contact with water. Besides, it should be non-toxic, abundant and easily processable into a desired shape. During the past 30 years, various inorganic semiconductors and molecular assemblies have been developed as catalysts for hydrogen production from water under visible light[1–12]. Semiconductors explored so far are constructed from transition-metal ions with d^0 electronic configuration or post-transition-metal ions of d^{10} configuration, along with group VA or VIA ions as counter-anion components[2,4–12]. For photocatalysis to be chemically productive, precious-metal species[11] such as Pt and RuO_2 must be used in most cases as extra cocatalysts to promote the transfer of photoinduced charge carriers from the bulk to the surface at which water is converted to hydrogen gas. Metal-based complexes (for example, a complex with four manganese ions in photosystem II (ref. 13) and a di-iron centre in hydrogenases[14]) are in natural enzymes the active sites photocatalysing the decomposition of water. Synthetic polymer semiconductors such as polyparaphenylene[15] have also been used for hydrogen production; however, they are active only in the ultraviolet region and have moderate performance. Here, we show that another simple polymer-like semiconductor, made of only carbon and nitrogen, can function as a metal-free photocatalyst for the extraction of hydrogen from water.

Carbon nitrides can exist in several allotropes with diverse properties, but the graphitic phase is regarded as the most stable under ambient conditions. The first synthesis of a polymeric carbon nitride, melon, was already reported by Berzelius and Liebig in 1834 (ref. 16), and it is therefore one of the oldest synthetic polymers reported. In recent work, we used the thermal polycondensation of common organic monomers to synthesize graphitic carbon nitrides (g-C_3N_4) with various architectures[17,18]. The graphitic planes are constructed from tri-*s*-triazine units connected by planar amino groups (Fig. 1a). The in-plane organization of tri-*s*-triazine units and the compression of aromatic planes were found to follow the perfection of condensation (see Supplementary Information, Figs S1,S2), enabling the generation of carbon nitride polymers with adjustable electronic properties, while keeping the free shapeability of a polymer made from liquid precursors. The carbon nitrides used in this study were prepared by heating cyanamide (Aldrich, 99% purity) to temperatures between 673 and 873 K (ramp: 2.2 K min^{-1}) for 4 h. For the material condensed at 823 K, an in-planar repeat period of 0.681 nm (for example, the distance of the nitride pores) in the crystal is evident from the X-ray powder diffraction (XRD) pattern (Fig. 1b), which is smaller than one tri-*s*-triazine unit (~0.713 nm), presumably owing to the presence of small tilt angularity in the structure. The strongest XRD peak at 27.4°, corresponding to 0.326 nm, is due to the stacking of the conjugated aromatic system, as in graphite (see Supplementary Information, Fig. S2). It should be noted that all of the materials feature some residual amount of hydrogen, which decreases with increasing condensation temperature.

Different thermal condensation enables the finer adjustment of the electronic and optical properties, as indicated by the ultraviolet–visible absorption spectrum for carbon nitrides prepared using different condensation temperatures (see Supplementary Information, Fig. S3). The absorption edge is moved towards longer wavelengths, indicating a decreasing bandgap with increasing condensation temperatures. The bandgap of the condensed graphitic carbon nitride is estimated to be 2.7 eV from its ultraviolet–visible spectrum (Fig. 1c), showing an intrinsic

[1]Max-Planck Institute of Colloids and Interfaces, Department of Colloid Chemistry, Research Campus Golm, 14424 Postdam, Germany, [2]Research Institute of Photocatalysis, State Key Laboratory Breeding Base of Photocatalysis, Fuzhou University, Fuzhou 350002, China, [3]Department of Chemical System Engineering, School of Engineering, The University of Tokyo, Bunkyo-ku, Tokyo 113-8656, Japan, [4]Fritz-Haber-Institute of the Max-Planck-Society, Theory Department, Faradayweg 4-6, D-14195 Berlin, Germany. *e-mail: xcwang@fzu.edu.cn; domen@chemsys.t.u-tokyo.ac.jp.

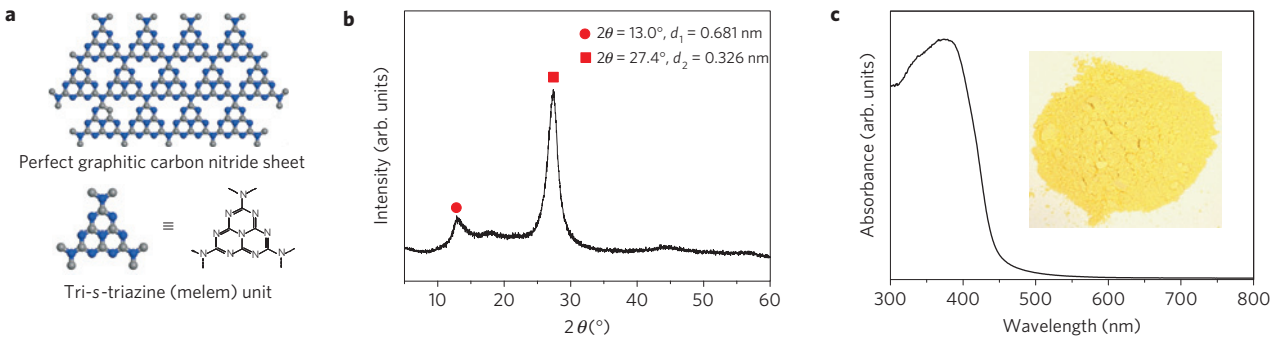

Figure 1 | Crystal structure and optical properties of graphitic carbon nitride. a, Schematic diagram of a perfect graphitic carbon nitride sheet constructed from melem units. **b**, Experimental XRD pattern of the polymeric carbon nitride, revealing a graphitic structure with an interplanar stacking distance of aromatic units of 0.326 nm. **c**, Ultraviolet–visible diffuse reflectance spectrum of the polymeric carbon nitride. Inset: Photograph of the photocatalyst.

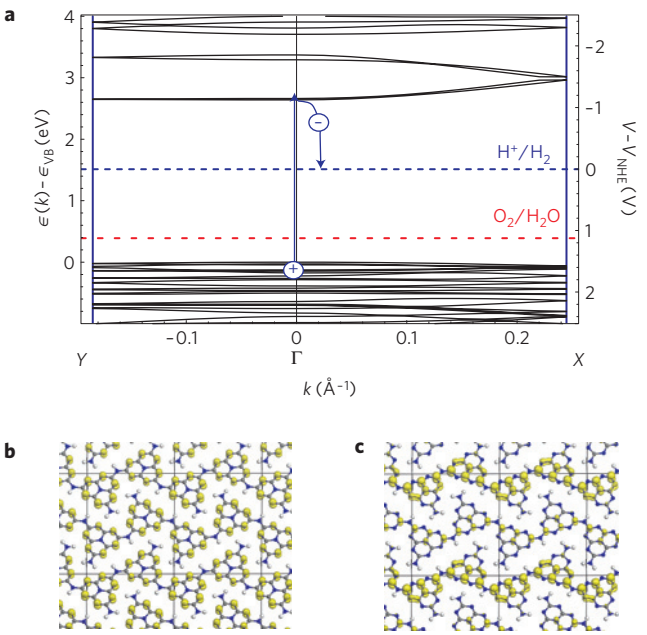

Figure 2 | Electronic structure of polymeric melon.
a, Density-functional-theory band structure for polymeric melon calculated along the chain (Γ–*X* direction) and perpendicular to the chain (*Y*–Γ direction). The position of the reduction level for H^+ to H_2 is indicated by the dashed blue line and the oxidation potential of H_2O to O_2 is indicated by the red dashed line just above the valence band. **b**, The Kohn–Sham orbitals for the valence band of polymeric melon. **c**, The corresponding conduction band. The carbon atoms are grey, nitrogen atoms are blue and the hydrogen atoms are white. The isodensity surfaces are drawn for a charge density of $0.01 q_e$ Å^{-3}.

semiconductor-like absorption in the blue region of the visible spectrum. This bandgap is sufficiently large to overcome the endothermic character of the water-splitting reaction (requiring 1.23 eV theoretically).

However, in addition to the magnitude of the bandgap, the character of the valence and conduction band and their absolute energies with respect to the reduction and oxidation levels are also important. To analyse the electronic structure, we have carried out density-functional-theory calculations[19] for different reaction intermediates along the condensation path in Supplementary Information, Fig. S1. The calculated bandgap decreases from the highest occupied molecular orbital/lowest unoccupied molecular orbital (HOMO–LUMO) gap in the melem molecule of 3.5 eV via 2.6 eV for polymeric melon[20] (Fig. 2) down to 2.1 eV for an infinite sheet of a hypothetically, fully condensed g-C_3N_4. Although the magnitude of the bandgap is underestimated, the trend in our calculations supports our interpretation of the ultraviolet–visible experiments. Figure 2a shows that the band structure of the recently suggested polymeric melon structure[20] has a non-isotropic band structure with a direct bandgap at the Γ point and only dispersion along the Γ–*X* direction parallel to the chain. The wavefunction of the valence band in Fig. 2b is a combination of the HOMO levels of the melem monomer, which are derived from nitrogen p_z orbitals. The conduction band can similarly be connected to the LUMO of the melem monomer, which consists predominantly of carbon p_z orbitals. Photoexcitation consequently leads to a spatial charge separation between the electron in the conduction band and the hole in the valence band. This suggests that the nitrogen atoms would be the preferred oxidation sites for H_2O to form O_2, whereas the carbon atoms provide the reduction sites for H^+ to H_2. We have finally calculated the absolute value of the reduction and oxidation levels for H_2O to check that they are both located inside the bandgap. The reaction energies were calculated with *ab initio* thermodynamics[21], where the free-energy contribution of the molecules was calculated in the ideal-gas approximation and the solvation energies for H^+ and H_2O were taken from the literature[22,23]. Our value for the reduction level of hydrogen $\mu_e^{H^+/H_2} = -4.18$ eV with respect to the vacuum level corresponds to an absolute value for the normal hydrogen electrode potential (NHE) $V_{NHE} = 4.18$ V. The calculated value for the oxidation level of H_2O, $\mu_h^{O_2/H_2O} = 5.30$ eV with respect to the vacuum level, corresponds to the oxidation potential $V_{O_2/H_2O} - V_{NHE} = 1.12$ V. Both of these values are slightly underestimated compared with experimental values $V_{NHE} = 4.44$ V and $V_{O_2/H_2O} - V_{NHE} = 1.23$ V (ref. 23). Figure 2a shows that the reduction level for H^+ is well positioned in the middle of the bandgap. This ascertains that the reduction process is energetically possible. The oxidation level is located slightly above the top of the valence band, which would permit transfer of holes, but presumably with a low driving force. These calculations provide evidence that carbon nitride has the potential to function as a photocatalyst for hydrogen production.

The photocatalysis experiments were carried out with g-C_3N_4 in powder form (Fig. 1c, inset) to provide sufficient surface area. It is insoluble in water as well as in acid (HCl, pH=0) or base (NaOH, pH = 14). The as-prepared g-C_3N_4 achieved steady H_2 production from water containing triethanolamine as a sacrificial electron donor on light illumination ($\lambda > 420$ nm) even in the absence of noble metal catalysts such as Pt, as shown in Fig. 3, curve (i). These results indicate that g-C_3N_4 functions as a stable 'metal-free' photocatalyst for visible-light-driven H_2 production.

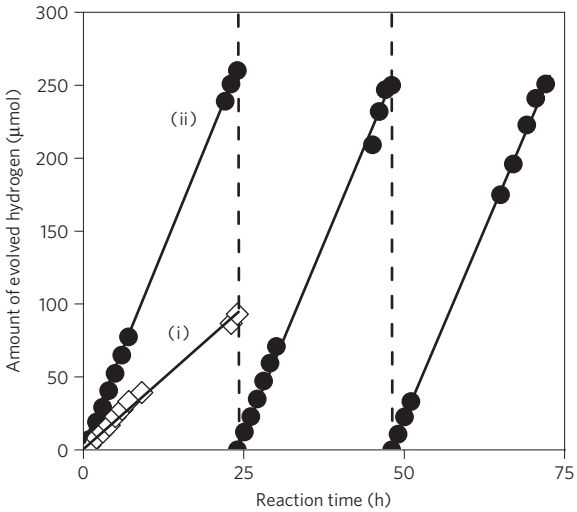

Figure 3 | Stable hydrogen evolution from water by g-C_3N_4. A typical time course of H_2 production from water containing 10 vol% triethanolamine as an electron donor under visible light (of wavelength longer than 420 nm) by (i) unmodified g-C_3N_4 and (ii) 3.0 wt% Pt-deposited g-C_3N_4 photocatalyst. The reaction was continued for 72 h, with evacuation every 24 h (dashed line). Unmodified g-C_3N_4 also photocatalysed steady H_2 production from aqueous methanol solution (10 vol%), as shown in Supplementary Information, Fig. S4.

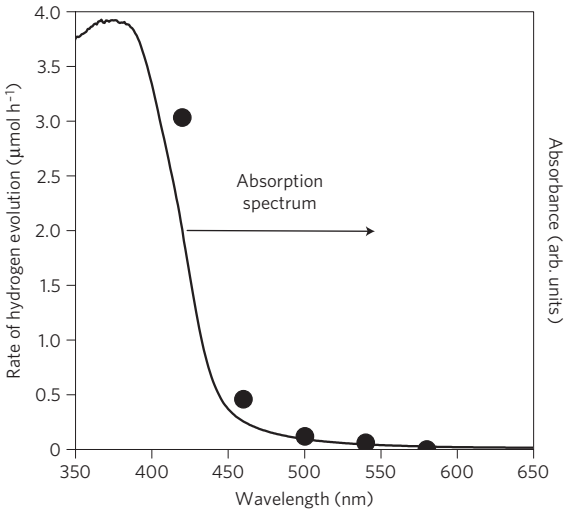

Figure 4 | Wavelength-dependent hydrogen evolution from water by g-C_3N_4. Steady rate of H_2 production from water containing 10 vol% methanol as an electron donor by 0.5 wt% Pt-deposited g-C_3N_4 photocatalyst as a function of wavelength of the incident light. Ultraviolet–visible absorption spectrum of the g-C_3N_4 catalyst is also shown for comparison.

However, the H_2 evolution activity of bare g-C_3N_4 was fluctuant, and exhibited variation from batch to batch (0.1–4 μmol h^{-1}). Modification with a small amount of Pt solved this problem, as described for other systems in the literature[24], improving activity and minimizing the experimental error to lie within 10–15% for different batch samples. This modification violates the 'metal-free' principle, but facilitates electron localization from the conduction band of g-C_3N_4 to the deposited Pt nanoparticles and simplifies H_2 production, here by about a factor of 7. We interpret this finding to be caused by the more favourable hydrogen elimination from Pt–H surface bonds, as compared with the covalent elimination from a hydrogenated g-C_3N_4 surface. Future work should focus on optimizing reaction conditions and improving surface area/surface functionality to catalyse hydrogen elimination even from the bare g-C_3N_4 to avoid the use of noble metals, which was however already shown to be possible.

The H_2 production rate increases with increasing Pt content to a plateau at around 2–4%, beyond which it decreases again. A typical time course of H_2 production using 3 wt% Pt-deposited g-C_3N_4 catalyst is shown in Fig. 3, curve (ii). The fact that the synthesized carbon nitride material contains residual hydrogen requires an evaluation of the origin of the hydrogen to exclude the possibility of the catalyst material as the hydrogen source. To evaluate stability, the reaction was allowed to proceed for a total of 72 h with intermittent evacuation every 24 h under visible-light irradiation ($\lambda > 420$ nm). Continuous H_2 evolution with no noticeable degradation of the carbon nitride was clearly observed from the beginning of the reaction. The total evolution of H_2 after 72 h was 770 μmol, by far exceeding the amount of surface C_6N_8 (tri-*s*-triazine) units (7.6 μmol) or the loaded Pt nanoparticles (15 μmol). (The number of surface C_6N_8 (tri-*s*-triazine) units is estimated to be 7.55×10^{-5} mol g^{-1} of g-C_3N_4. The calculation is based on the specific surface area of g-C_3N_4 ($\sim 10\ m^2\ g^{-1}$), which was determined by the Brunauer–Emmett–Teller method at liquid-nitrogen temperature, and the area of C_6N_8 units ($\sim 0.22\ nm^{-2}$).) To confirm that hydrogen is not coming from g-C_3N_4, we carried out an extra experiment using Pt/g-C_3N_4 under ultraviolet light ($\lambda > 300$ nm). The system steadily produced 4.5 mmol H_2 in 19 h, exceeding the amount of hydrogen (1 mmol) in the catalyst. In most cases where nitrogen-containing materials (for example, (oxy)nitrides) are used as photocatalysts, a low level of N_2 evolution is detected in the initial stage of photocatalytic reaction[6]. This is attributed to the oxidation of N^{3-} species near the material surface to N_2. No N_2 evolution was observed for the present catalyst even after the extended period of irradiation, which may indicate strong binding of N in the covalent carbon nitride. These results indicate excellent stability of the present material for photocatalytic H_2 production. Production of H_2 was also observed when other electron donors including methanol, ethanol and ethylenediaminetetraacetic acid were used instead of triethanolamine, although the hydrogen evolution rates were lower (see Supplementary Information, Fig. S5).

To support that reaction proceeds through light absorption within the carbon nitride polymer, we also examined the dependence of the rate of H_2 evolution on the wavelength of incident light. As shown in Fig. 4, the trend of H_2 evolution rates matches well with that of absorption in the optical spectra. The longest wavelength available for the reaction is 540 nm, which corresponds to the absorption edge of the catalyst. A control experiment showed that indeed no reaction took place in the dark.

It is not the most condensed material (condensed at 873 K) that shows the highest activity, but the more polymeric C_3N_4 material condensed at 823 K. Obviously, some defect structures are crucial, presumably to localize the electron and hole at specific surface termination sites where they can be transferred to the water molecules.

Note that although hydrogen generation from water is an achievement, it constitutes only the minor half of the problem of water splitting. Water oxidation by non-oxide catalysts remains the real challenge of the community. For inorganic sulphides and (oxy)nitrides, the anion components are less stable and, in some cases, more susceptible to oxidation than water. There are some cases where N_2 evolution and sulphur deposition are observed as a result of oxidative decomposition of the photocatalyst[25]. Indeed, our system in the previous experiments did not eliminate molecular oxygen (presumably again because of the covalent character of the

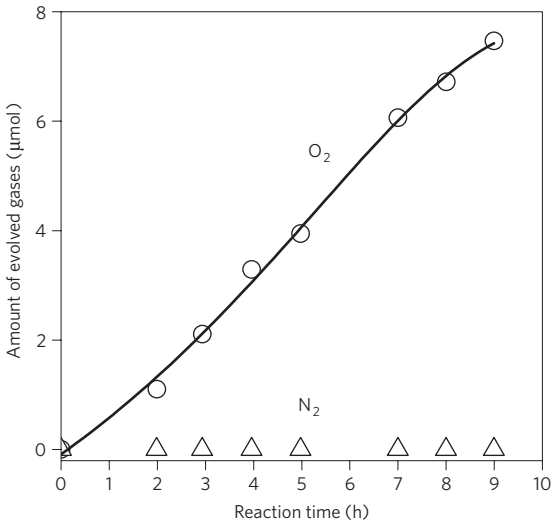

Figure 5 | Oxygen evolution from water by g-C_3N_4. Time courses of O_2 production from water containing 0.01 M silver nitrate as an electron acceptor under visible light (of wavelength longer than 420 nm) by 3.0 wt% RuO_2-loaded g-C_3N_4. La_2O_3 (0.2 g) was used as a buffer (pH 8–9).

oxygen bonds), and a sacrificial reactant to take up the oxygen was used. The bandgap calculations however indicate that in principle oxygen elimination should be thermodynamically possible, as the HOMO was found to lie below the water oxidation potential.

This stimulates further research for constructing a suitable catalytic active site that efficiently promotes O_2 evolution from the g-C_3N_4 surface. As a first trial, we thus attempted to introduce RuO_2, which is well known as a good oxidation catalyst for O_2 evolution[26–28], by an impregnation method[12], using silver nitrate as a sacrificial electron acceptor.

As shown in Fig. 5, the modified catalyst exhibited visible-light activity ($\lambda > 420$ nm) for O_2 evolution with no N_2 evolution, although the activity for O_2 evolution was an order of magnitude lower than that for H_2 evolution (Fig. 3). These results indicate that the loaded RuO_2 is able to take up the photogenerated holes from g-C_3N_4, exhibiting functionality as efficient O_2 evolution sites. The decrease in activity with reaction time is primarily attributable to the deposition of metallic silver on the catalyst surface, which blocks light absorption and obstructs active sites[6,7]. Under ultraviolet irradiation ($\lambda > 300$ nm), the amount of O_2 evolved for 8 h reaction reached 53 μmol (see Supplementary Information, Fig. S6), which is larger than that in the RuO_2 catalyst (about 28 μmol). (The amount of O_2 in the RuO_2 (3.0 wt%)-loaded g-C_3N_4 (0.1 g) is calculated to be about 28 μmol. It should be noted that g-C_3N_4 contains oxygen species as impurities at a rate of about 0.2 wt%.) This fact clearly demonstrates that the observed O_2 evolution is no doubt derived from water oxidation. The low activity for O_2 evolution can be explained by the band-structure calculation, which showed that the thermodynamic driving force of g-C_3N_4 for O_2 evolution is much smaller than that for H_2 evolution (Fig. 3). Although the present preliminary results can be regarded as promising, further optimization for the O_2 evolution system is thus needed.

In summary, we presented here polymeric carbon nitride as a commonly available and simple photocatalyst that is able to generate hydrogen from water even in the absence of noble metals. Although the estimated quantum efficiency of the Pt-modified C_3N_4 catalyst is still rather low (approximately 0.1% with irradiation of 420–460 nm (Fig. 4)), the present result opens new vistas for the search of energy production schemes, using thermally and oxidation-stable polymeric organic semiconductor structures as the functional material that are cheap and commonly available.

Received 21 April 2008; accepted 8 October 2008; published online 9 November 2008

References

1. Borgarello, E. *et al.* Photochemical cleavage of water by photocatalysis. *Nature* **289**, 158–160 (1981).
2. Kim, Y. I., Salim, S., Huq, M. J. & Mallouk, T. E. Visible-light photolysis of hydrogen iodide using sensitized layered semiconductor particles. *J. Am. Chem. Soc.* **113**, 9561–9563 (1991).
3. Khaselev, O. & Turner, J. A. A monolithic photovoltaic-photoelectrochemical device for hydrogen production via water splitting. *Science* **280**, 425–427 (1998).
4. Sayama, K. *et al.* Stoichiometric water splitting into H_2 and O_2 using a mixture of two different photocatalysts and an IO_3^-/I^- shuttle redox mediator under visible light irradiation. *Chem. Commun.* 2416–2417 (2001).
5. Kato, H. & Kudo, A. Visible-light-response and photocatalytic activities of TiO_2 and $SrTiO_3$ photocatalysts codoped with antimony and chromium. *J. Phys. Chem. B* **106**, 5029–5034 (2002).
6. Hitoki, G. *et al.* An oxynitride, TaON, as an efficient water oxidation photocatalyst under visible light irradiation ($\lambda \leq 500$ nm). *Chem. Commun.* 1698–1699 (2002).
7. Ishikawa, A. *et al.* Oxysulfide $Sm_2Ti_2S_2O_5$ as a stable photocatalyst for water oxidation and reduction under visible light irradiation ($\lambda \leq 650$ nm). *J. Am. Chem. Soc.* **124**, 13547–13553 (2002).
8. Tsuji, I., Kato, H., Kobayashi, H. & Kudo, A. Photocatalytic H_2 evolution reaction from aqueous solutions over band structure-controlled $(AgIn)_xZn_2(1-x)S_2$ solid solution photocatalysts with visible-light response and their surface nanostructures. *J. Am. Chem. Soc.* **126**, 13406–13413 (2004).
9. Tsuji, I., Kato, H. & Kudo, A. Visible-light-induced H_2 evolution from an aqueous solution containing sulfide and sulfite over a ZnS–$CuInS_2$–$AgInS_2$ solid-solution photocatalyst. *Angew. Chem. Int. Ed.* **44**, 3565–3568 (2005).
10. Maeda, K. *et al.* GaN:ZnO solid solution as a photocatalyst for visible-light-driven overall water splitting. *J. Am. Chem. Soc.* **127**, 8286–8287 (2005).
11. Maeda, K. *et al.* Photocatalyst releasing hydrogen from water—Enhancing catalytic performance holds promise for hydrogen production by water splitting in sunlight. *Nature* **440**, 295 (2006).
12. Lee, Y. *et al.* Zinc germanium oxynitride as a photocatalyst for overall water splitting under visible light. *J. Phys. Chem. C* **111**, 1042–1048 (2007).
13. Yachandra, V. K. *et al.* Where plants make oxygen—a structural model for the photosynthetic oxygen-evolving manganese cluster. *Science* **260**, 675–679 (1993).
14. de Carcer, I. A., DiPasquale, A., Rheingold, A. L. & Heinekey, D. M. Active-site models for iron hydrogenases: Reduction chemistry of dinuclear iron complexes. *Inorg. Chem.* **45**, 8000–8002 (2006).
15. Yanagida, S., Kabumoto, A., Mizumoto, K., Pac, C. & Yoshino, K. Poly(para)phenylene-catalyzed photoreduction of water to hydrogen. *JCS-Chem. Commun.* **8**, 474–475 (1985).
16. Liebig, J. About some nitrogen compounds. *Ann. Pharm.* **10**, 10 (1834).
17. Groenewolt, M. & Antonietti, M. Synthesis of g-C_3N_4 nanoparticles in mesoporous silica host matrices. *Adv. Mater.* **17**, 1789–1792 (2005).
18. Goettmann, F., Fischer, A., Antonietti, M. & Thomas, A. Chemical synthesis of mesoporous carbon nitrides using hard templates and their use as a metal-free catalyst for Friedel-Crafts reaction of benzene. *Angew. Chem. Int. Ed.* **45**, 4467–4471 (2006).
19. Clark, S. J. *et al.* First principles methods using CASTEP. *Z. f Krist* **220**, 567–570 (2005).
20. Lotsch, B. V. *et al.* Unmasking melon by a complementary approach employing electron diffraction, solid-state NMR spectroscopy, and theoretical calculations-structural characterization of a carbon nitride polymer. *Chem. Eur. J.* **13**, 4969–4980 (2007).
21. Reuter, K. & Scheffler, M. Composition, structure, and stability of $RuO_2(110)$ as a function of oxygen pressure. *Phys. Rev. B* **65**, 035406 (2001).
22. Tissandier, M. D. *et al.* The proton's absolute aqueous enthalpy and Gibbs free energy of solvation from cluster-ion solvation data. *J. Phys. Chem. A* **102**, 7787–7794 (1998).
23. Weast, R. C., Astle, M. J. & Beyer, W. H. *Handbook of Physics and Chemistry* 64th edn, D158 (CRC Press, 1983).
24. Kraeutler, B & Bard, A. J. Heterogeneous photocatalytic preparation of supported catalysts—photodeposition of platinum on TiO_2 powder and other substrates. *J. Am. Chem. Soc.* **100**, 4317–4318 (1978).
25. Maeda, K. & Domen, K. New non-oxide photocatalysts designed for overall water splitting under visible light. *J. Phys. Chem. C* **111**, 7851–7861 (2007).
26. Kalyanasundaram, K. & Grätzel, M. Cyclic cleavage of water into H_2 and O_2 by visible light with coupled redox catalysts. *Angew. Chem. Int. Ed.* **18**, 701–702 (1979).
27. Borgarello, E., Kiwi, J., Pelizzetti, E., Visca, M. & Grätzel, M. Photochemical cleavage of water by photocatalysis. *Nature* **289**, 158–160 (1981).

28. Harriman, A., Pickering, I. J., Thomas, J. M. & Christensen, P. A. Metal oxides as heterogeneous catalysts for oxygen evolution under photochemical conditions. *J. Chem. Soc. Faraday Trans. 1* **84**, 2795–2806 (1988).

Acknowledgements

This work was supported by the Max Planck Society within the framework of the project ENERCHEM, and the Research and Development in a New Interdisciplinary Field Based on Nanotechnology and Materials Science programs of the Ministry of Education, Culture, Sports, Science and Technology (MEXT) of Japan. X.W. is grateful for the financial support from the National Basic Research Program of China (973 program, Grant No. 2007CB613306), NSFC (Grant Nos. 20537010 and 20603007), the New Century Excellent Talents in University of China (NCET-07-0192) and the AvH Foundation. K.M. gratefully acknowledges the support of a Japan Society for the Promotion of Science (JSPS) Fellowship. The authors thank J. Kubota, T. Hisatomi and K. Kamata (Department of Chemical System Engineering, The University of Tokyo) for assistance in the revision of this article.

Additional information

Supplementary Information accompanies this paper on www.nature.com/naturematerials. Reprints and permissions information is available online at http://npg.nature.com/reprintsandpermissions. Correspondence and requests for materials should be addressed to K.D. or X.C.W.